Journal of Inorganic and Organometallic Polymers and Materials (2023) 33:3750–3759
https://doi.org/10.1007/s10904-023-02744-3

RESEARCH

Novel Green Synthesis of UV-Sunscreen ZnO Nanoparticles Using *Solanum Lycopersicum* Fruit Extract and Evaluation of Their Antibacterial and Anticancer Activity

Aya Elbrolesy[1] · Y. Abdou[2] · F. A. Elhussiny[1] · Reda Morsy[1]

Received: 11 May 2023 / Accepted: 30 May 2023 / Published online: 14 June 2023

Abstract
This work aimed at the green synthesis of multifunctional zinc oxide nanoparticles (ZnO NPs) using *Solanum Lycopersicum* (SL) fruit juice to act as antibacterial/cancer/UV sunscreens. The obtained ZnO NPs were examined for optical properties, cytotoxicity of human lung fibroblast (WI-38) and hepatocellular carcinoma (HePG2) cell lines, and antibacterial activity against Gram-negative *Escherichia coli* and Gram-positive *Staphylococcus aureus*. The antioxidant activity and in vitro sun protection factor (SPF) of the synthesized nanoparticles were carried out by spectrophotometric methods. The formation of pure phase structure and characteristic functional group of the synthesized ZnO NPs were confirmed by XRD, FTIR, and UV–Vis diffuse reflectance analysis. SEM image showed that the ZnO NPs have a quasi-spherical shape with a size of about 39 ± 12 nm. ZnO NPs showed high potency as sunscreens (in vitro SPF = 16.8) and as mild antioxidant agents. Notably, ZnO NPs enhanced the cytotoxic activity against hepatocellular carcinoma cells and confirmed their antibacterial activity against pathogenic bacteria. SL fruit juice can play a triple role by acting as a solvent, reducing agent and stabilizer which facilitates the synthesis of ZnO NPs sunscreen that has antibacterial and anti-carcinogenic properties.

Keywords ZnO nanoparticles · Sunscreen · Green synthesis · Anticancer · Antibacterial · *Solanum*

1 Introduction

The increased exposure of human skin to the sun's ultraviolet rays and their penetration into the deeper layers of the skin may lead to risks ranging from skin discoloration to skin aging to skin cancer, as well as increased activity of pathogens when the skin is infected [1–3]. Among the many sunscreens suggested by the scientific community, inorganic sunscreens, such as ZnO NPs, are a regular protection against UV radiation [4]. Over the past decade, several studies have shown promising results for ZnO NPs in several biomedical applications, including sunscreen agents, biosensors, antitumor, antibacterial activity, and antioxidants [5]. As sunscreen agents, small sized zinc oxide particles have a significant attenuating effect on ultraviolet B (UVB) radiation, as UVB rays are scattered, absorbed and reflected, enabling them to act as a physical barrier to protect the stratum corneum of the skin [6]. ZnO NPs are highly valued biological nanomaterials due to their non-toxicity, biocompatibility, photocatalytic activity, high stability, and biodegradability [7, 8]. Moreover, zinc oxide can overcome pathogenic bacteria that have antibiotics-resistance, and it has fewer side effects compared to organic sunscreens [9, 10]. Several chemical, physical and biological (green) synthesis approaches have been used to synthesize ZnO NPs with desired shape and sizes [11, 12]. However, both chemical and physical methods are subject to several drawbacks, including prohibitive costs, time consumption, high energy consumption, and the use of toxic and hazardous chemicals, which are not environmentally friendly [11–13]. Currently, the interest in using green synthesis to synthesize ZnO NPs has increased due to it being a simple, low-cost, sustainable and eco-friendly method [14]. As such, compared to traditional chemical methods for the synthesis of ZnO NPs, green synthesis has become an important approach to reduce negative impacts on the environment because it does not use any

✉ Aya Elbrolesy
ayamelbrolesy@gmail.com

[1] Biophysics Lab, Physics Department, Faculty of Science, Tanta University, Tanta 31527, Egypt

[2] High Energy Physics Lab, Physics Department, Faculty of Science, Tanta University, Tanta 31527, Egypt

environmentally harmful substances as reactants, nor does it produce any environmentally harmful substances as reactants [15, 12]. Moreover, the use of green synthesis method involving plant synthesis of ZnO NPs is a promising method because it is cost-effective, rapid, one-step, and biocompatible [16]. Green synthesis approach of ZnO NPs is based on the possibility of using various active substances of plants and microorganisms as reducing agents, capping agents and solvent systems [17]. The microorganisms used in the green synthesis of ZnO NPs included bacteria [15, 18, 19], fungi [20, 21], and algae [22], and on the other hand, the plant extracts included roots, stems, leaves [23–25] and fruits [26]. Among them, plant extracts are preferred for the synthesis of ZnO NPs because they are simple and easy to prepare and enable large-scale production of nanoparticles [14–17]. Several plants have been extensively tested for active materials suitable for the green synthesis of ZnO NPs, especially those rich in active substances capable of reducing and stabilize zinc salts into zinc oxide nanoparticles [27, 28]. Generally, the initial solution of zinc is mixed with plant extracts under appropriate reaction conditions including pH, temperature, pressure, and concentration [29]. Moreover, it can add therapeutic efficacy to synthetic molecules, enhancing their antibacterial or anticancer activity [30, 31]. Also, when biomolecules such as salts, amino acids, phytochemicals, and proteins present in plant extracts are added to ZnO NPs during the synthesis process, it can make the ZnO NPs more biocompatible and effective within living tissues because of their biochemical similarity to cellular components responsible for cell growth [32, 33]. *Solanum Lycopersicum* (SL) is a seasonal plant (tomato), and they are one of the most important daily foods in addition to its important medicinal properties, due to the presence of carotenoids (such as lycopene), polyphenols (such as flavanones and anthocyanidins), and ascorbic acid which are antioxidants and anticarcinogens [34]. Lycopene is a red carotenoid that has antioxidant and anti-inflammatory properties, in addition to preventing cancer, as it was found that it can accumulate in the prostate and enhance its protection against prostate cancer [35]. Lycopene as an oxidizing agent can prevent oxidative damage to DNA and the potential conversion of normal cells into cancer cells through the quenching of single oxygen and scavenging of free radicals [36]. Thus, all components of SL fruit extract together with their antioxidant and anticancer properties make SL extract of promising utility in the prevention and control of cancer [37]. This work aims to develop more effective and multifunctional ZnO NPs sunscreens to provide integrated protection where the combination of antibacterial, antitumor activity and UV protection can improve the efficacy of sunscreens due to synergistic effects. In this regard, the green synthesis of ZnO nanoparticles was used due to it being an economical, environmentally friendly and safe method for the synthesis of toxin-free ZnO. The toxicity factor of raw ingredients is particularly important when used in cosmetics. Here, we developed a novel approach for the green synthesis of UVB sunscreen ZnO NPs using SL fruit juice to investigate its synergistic effect on pathogenic bacteria (Gram-negative *Escherichia coli* and Gram-positive *Staphylococcus aureus*) and on normal (Human lung fibroblast) and cancerous (Hepatocellular carcinoma) cell lines. In this study, ZnO NPs were eco-friendly and synthesized using SL fruit juice (green synthesis). The structure, composition, morphology, and optical properties of ZnO NPs were determined using XRD, FTIR, FSEM, and UV–Vis diffuse reflectance analysis. The effects of ZnO NPs were evaluated against normal (Human lung fibroblast) and cancerous (Hepatocellular carcinoma) cell lines and on pathogenic bacteria (Gram-negative *Escherichia coli* and Gram-positive *Staphylococcus aureus*) were investigated. The antioxidant activity and in vitro sun protection factor (SPF) of the synthesized nanoparticles were carried out by spectrophotometric methods.

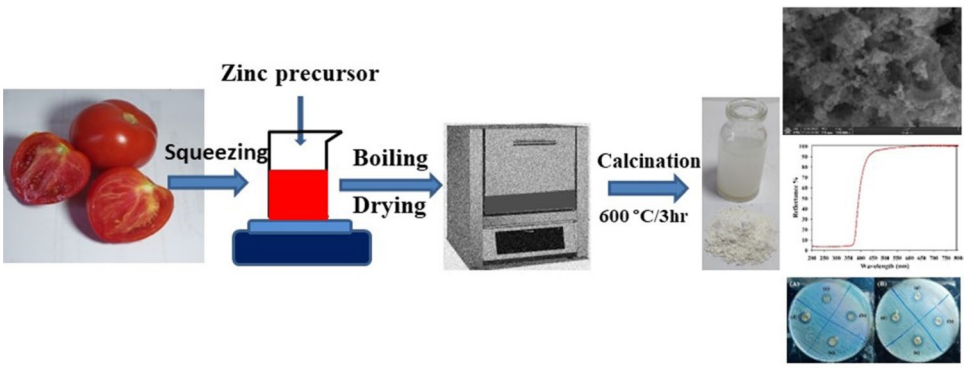

2 Experimental Methods

2.1 Materials and Reagents

Solanum Lycopersicum (SL) was determined using classification keys. The healthy and ripe fruits were purchased from the local vegetable market in Tanta, Gharbia Governorate, Egypt. Zinc nitrate hexahydrate ($Zn(NO_3)_2.6H_2O$ was purchased from Oxford Lab, India: purity 96%). Cell lines: human lung fibroblast (WI-38) and human hepatocellular carcinoma (HepG2) cells were obtained from VACSERA (Cairo, Egypt). Roswell Park Memorial Institute-1640 (RPMI-1640) was purchased from Lonza Inc. (USA). Fetal bovine serum (FBS was purchased from GIBCO, UK:

impurities ≤ 10 EU/mL endotoxin). Dimethyl sulfoxide (DMSO, purity 99.9%), 1,1-diphenylpicrylhydrazyl (DPPH, purity 97%), and Dimethyl-2-thiazolyl-2,5-diphenyl-2 H-tetrazolium bromide (MTT, purity ≥ 98%) assay were purchased from Sigma Aldrich (USA). Absolute ethanol was purchased from El-Naser Co. (Egypt, purity ≥ 99.5%).

2.2 Preparation of Fruit Juice of Solanum Lycopersicum and Synthesis of ZnO NPs

To prepare SL fruit juice, fresh SL fruits were washed several times with distilled water, then peeled, squeezed in an electric blender at room temperature and filtered. The green synthesis of ZnO NPs was carried out by solution combustion method using zinc precursor and SL extract as biofuel. An amount (19.0 g) of $Zn(NO_3)_2.6H_2O$ was completely dissolved in 40 mL of distilled water and then mixed and stirred with 140 mL of SL juice until a homogeneous solution was formed. The mixture was boiled on a hot plate to evaporate the water and obtain dry foam. When the foam reached the point of spontaneous combustion, it began to burn and formed a grayish-white powder. The obtained powder was calcinated at 600 °C for 3 h in an electric oven.

2.3 Characterization Techniques

The crystal structure and phase composition of the synthesized sample were investigated by using powder X-ray diffraction (XRD). The XRD patterns were done using an X-ray diffractometer (Bruker-D8 Advance, Germany) over the range of 2theta (20°−80°) with Cu/Kα radiation (λ = 1.5418 Å). The Joint Committee for Powder Diffraction Standards (JCPD card No. 36-1451) for standard ZnO peak positions was used to identify the crystal phases for the sample. The crystal size of ZnO sample was calculated using the Debye-Scherer equation ($D = k\lambda/\beta\cos\theta$) where D is the average crystal size, K is a constant (0.93), λ is the X-ray wavelength, β is the full width at half-maximum of the studied peak, and θ is the Bragg angle [9]. Morphological and microstructural analysis of the formed nanoparticles was performed using a field emission scanning electron microscope (FESEM: JEOL JSM 6510 IV) at which the scanning scales were set to 120,000×. ImageR software was used to calculate the mean nanoparticle size from the FE-SEM images by counting 100 calibrated particles. Fourier transform infrared spectroscopy (FITR: Jasco FT/IR-400) was used to investigate the chemical composition of the synthesized ZnO nanoparticles. The spectrum was recorded in the region 400–4000 cm^{-1} with a spectral resolution of 4 cm^{-1}.

2.4 Optical Properties and Sun Protection Factor (SPF) of ZnO NPs

The optical absorption properties of solid powders of ZnO NPs were characterized by using ultraviolet-visible diffuse reflectance spectroscopy (DRS: Shimadzu UV-2050) while barium sulfate was used as a reference. The spectrum was recorded in the wavelength range from 200 to 800 nm at room Temperature. UV–Visible spectroscopy (Labomed UVS-2700) was used to investigate the in vitro sun protection factor (SPF) of ZnO NPs. The spectrum of absorbance measurements was recorded over a wavelength range of 290–320 nm every 5 nm. One gram of ZnO NPs was dispersed in 100 mL of absolute ethanol at room temperature. The following Mansur equation [38] was used to calculate the SPF value of synthesized ZnO NPs:

$$\mathrm{SPF} = \mathrm{CF} \sum_{290}^{320} \mathrm{A}(\lambda)\, \mathrm{I}(\lambda)\, \mathrm{EE}(\lambda) \quad (1)$$

where CF = 10 is the correction factor, A is the ZnO NPs absorbance, λ is the wavelength, I is the solar intensity spectrum, and EE is the erythemal effect.

2.5 Antioxidant Activity: DPPH Radical Scavenging Activity Assay

The DPPH test was used to determine the antioxidant capacity of ZnO NPs in a spectrophotometric manner at OD_{517} nm while ascorbic acid was used as a standard (control). Different concentrations of ZnO NPs suspensions (10, 20, 40, 60, 80, and 100 μg/mL) were dispersed in methanol. According to the following formula, used to evaluate the ability of ZnO NPs to scavenge DPPH free radicals, the highest amount of DDPH is 100%.

$$\text{Percentage of DPPH scavenging activity}(\%) = 100 \times \frac{\text{control OD} - \text{ZnO sample OD}}{\text{control OD}} \quad (2)$$

2.6 Antibacterial Activity

The agar-well diffusion method was used to evaluate the antibacterial activity of green synthetic ZnO NPs against Gram-negative (*Escherichia coli)* and Gram-positive (*Staphylococcus aureus)* bacteria. Stock suspensions of ZnO NPs (0.25, 0.5, 1, and 2 mg/mL) were prepared by ultrasonically dispersing them in sterile water. The nutrient broth at 37 °C was used to grow pure cultures of bacteria for 24 h. Sterile cotton swabs were used to swap each strain homogenously onto each plate. Inverted micro tips (6 mm) were used to prepare the wells and the dispersed ZnO NPs were poured into each well while sterile water was used as a negative control. Agar plates were incubated at 37 °C for 24 h and the diameters of the inhibition zone were measured to evaluate the antibacterial activities.

2.7 Cell Culture and Cytotoxic Evaluations

Cell lines (WI-38 and HepG2) were cultured in RPMI medium, 10% FBS, and antibiotics (100 units/mL penicillin and 100 µg/mL streptomycin) at 37 °C in a 5% carbon dioxide incubator. The MTT assay was used to evaluate the cytotoxic activity of the ZnO NPs with cell lines. 100 µl of cell lines (density of 1×10^4) were seeded in a 96-well plate at 37 °C and incubated for 48 h in a controlled humidified atmosphere (95% air and 5% CO_2). Different concentrations of ZnO NPs suspensions (0, 1.56, 3.125, 6.25, 12.5, 25, 50, and 100 µg/mL) were mixed with the cells and the incubation was continued for 24 h in a humidified atmosphere (95% air and 5% CO_2). Then 20 µl of MTT solution (0.5 mg/mL in PBS) was added into each well and incubated for 4 h, then 100 µl of DMSO was added to dissolve the formed MTT formazan. For the measurement and recording of the colorimetric assay, a plate reader (EXL 800, USA) with an absorbance of 570 nm was used. The following formula was used to calculate the percentage of viable cells (viability (%)):Viability(%) = test/control × 100.

3 Results and Discussion

SL fruit juice is an excellent, non-toxic source for synthesizing ZnO NPs. It can play a triple role by acting as a solvent, reducing agent and stabilizer which facilitates the synthesis of ZnO NPs. SL fruit juice has a high water content that can be used as a solvent system for the green synthesis of ZnO NPs. Water is the ideal solvent system for chemical reactions because it is non-toxic and inexpensive [39]. A potential reaction mechanism for the green synthesis of ZnO NPs emerges from the interaction potential between zinc nitrate and the nutritional and functional active constituents of *solanum lycopersicum* (Fig. 1), including organic acids

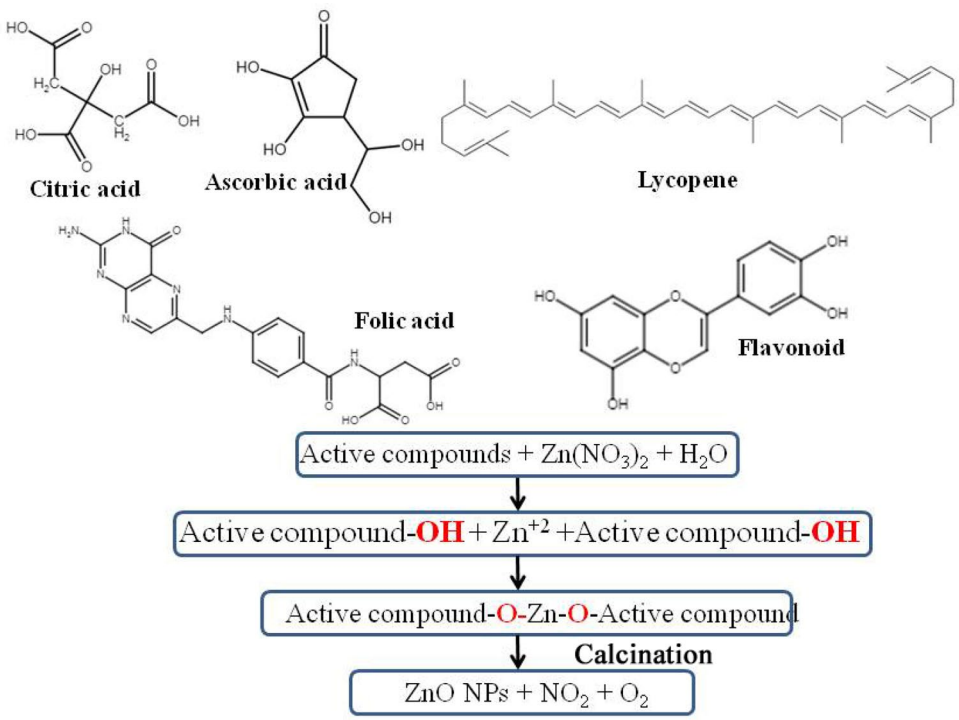

Fig. 1 Bioactive compounds of SL fruit juice and the synthesis mechanism of ZnO NPs

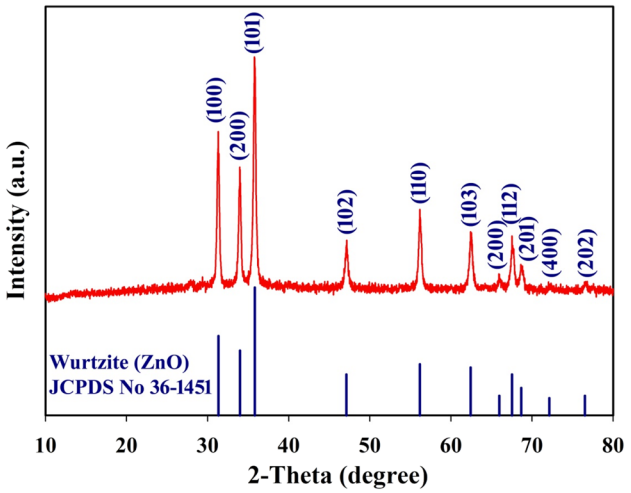

Fig. 2 XRD pattern of ZnO NPs calcined at 600 °C temperature for 3 h using SL juice

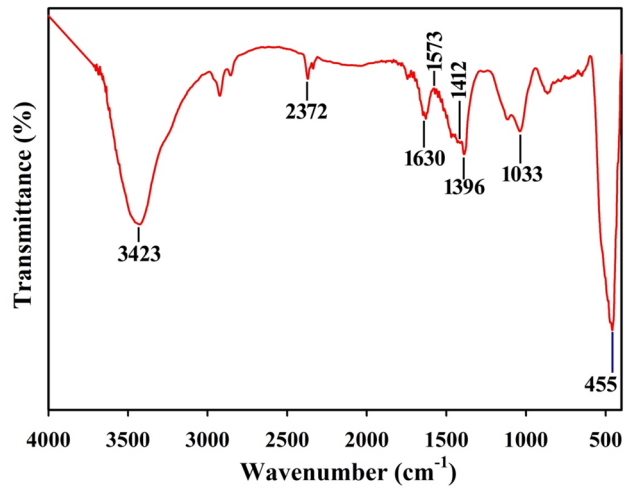

Fig. 3 FTIR spectrum of ZnO NPs calcined at 600 °C temperature for 3 h using SL juice

such as citric, ascorbic, and folic acid as well as carotenoids, and flavonoids have the ability to bioreduce zinc ions [40]. These active biomolecules acted as reducing as well as stabilizing agent for the green synthesis of ZnO NPs [41]. During the reaction, zinc ions can form complex agents with aromatic hydroxyl groups of biomolecules and then start the nucleation process as shown in Fig. 1, which then leads to reduction and formation of ZnO NPs. Calcination at 500 °C can decompose the complex system and release ZnO NPs directly [42].

3.1 Characterization of ZnO NPs

Figure 2 shows the XRD pattern of ZnO prepared by green synthesis. Compared to the standard PDF (JCPD Card No. 36-1451), all XRD reflections of synthesized ZnO can only be indexed to one phase (wurtzite ZnO). The peaks observed at $2\theta = 31.5°$, 34°, 36°, 47°, 56°, 62.5°, 66°, 67.5°, 68.5°, 72°, and 76.5° are assignable to the hexagonal wurtzite structure of ZnO. The XRD pattern confirms that the synthesized ZnO is a pure phase as no secondary phases or contaminations were detected. Using the Scherer's formula, the average crystal size of the synthesized ZnO NPs was estimated to be approximately 23 nm. The cosmetic properties of zinc oxide as an inorganic sunscreen depend on the particle size, the lower the particle size on the nanoscale (< 100 nm), the higher the UV scattering capabilities [43].

Figure 3 shows the characteristic FTIR spectrum of the functional groups of ZnO NPs in the wave number range of 400–4000 cm^{-1} [44]. The Zn-O bond stretching vibration mode has an absorption band of 455 cm^{-1} [45]. The absorption peaks of 3423 cm^{-1} and 1630 cm^{-1} of the nanoparticles represent the vibrational stretching and bending modes of the O–H bond of water, respectively [46]. The carboxylate bond stretching vibration (C=O) of symmetric and asymmetric zinc has an absorption band in the region around 1412 cm^{-1} and 1573 cm^{-1} [47]. Furthermore, the

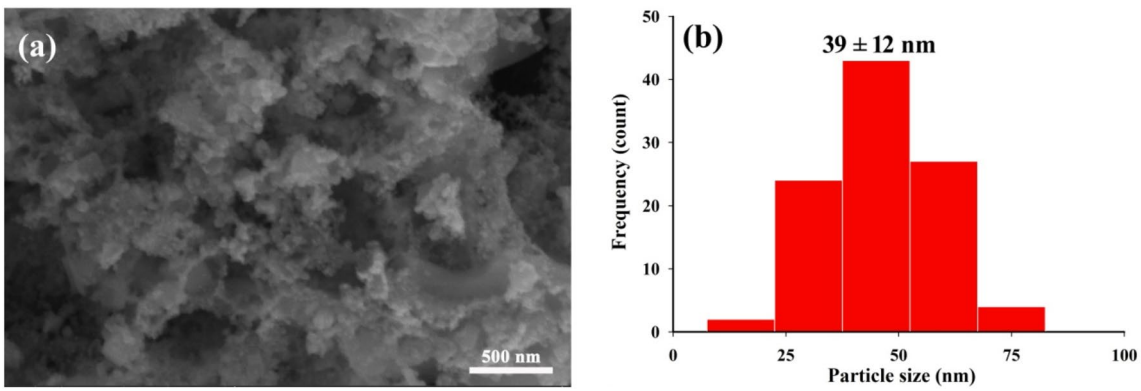

Fig. 4 FESEM image (**a**) and particle size distribution (**b**) image for ZnO NPs

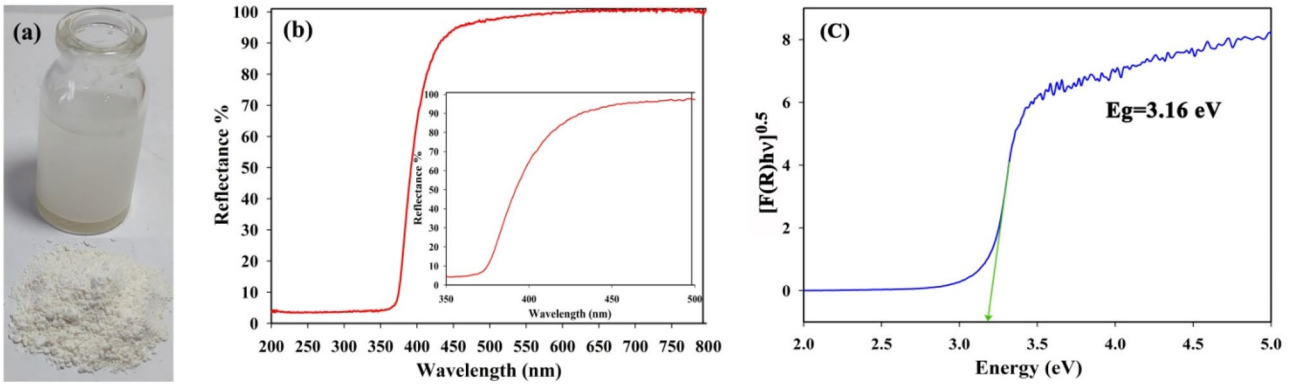

Fig. 5 Optical properties of ZnO NPs: **a** white color of ZnO NPs, **b** UV–visible diffuse reflectance spectra of ZnO NPs (inset: zoomed in spectra in the range from 350 to 500 nm), and **c** Plot of $[F(R)h\nu]^{0.5}$ against photon energy ($h\nu$)

Table 1 The normalized EE(λ)×I(λ) used in the calculations and SPF values of ZnO NPs

Wavelength (nm)	EE(λ)×I(λ)
290	0.0150
310	0.1964
315	0.0939
320	0.0180
Samples	**SPF value**
ZnO	16.8

Table 2 DPPH radical scavenging activity of synthesized ZnO NPs and ascorbic acid

Concentration (µg/ml)	Scavenging ability (%)	
	ZnO	Ascorbic acid
10	13.4	38.7
20	23.9	52.1
40	33.6	69.6
60	53.1	81.8
80	67.7	87.4
100	75.1	94.5
IC50 value (µg/ml)	51.91 ± 0.29	16.81 ± 0.10

characterization of the CO_2 bond peak in the air appeared at 2376 cm^{-1} [48].

Figure 4 shows the topological features (morphology, size, and microstructure) of ZnO NPs as investigated by FESEM. FESEM image revealed the formation of ZnO NPs with quasi-spherical shapes, and the size is about 39 ± 12 nm.

3.2 Optical Properties and Sun Protection Factor Performance of ZnO NPs

Figure 5 shows the white color (a), the diffuse reflectance spectra (b), and band gap plot (c) of ZnO NPs green synthesized using SL juice used in sunscreen applications. The UV–visible diffused reflectance spectrum showed very low reflectance values of ZnO NPs in the entire UV region (280–3700 nm). This UV range includes the entire UV-B region (280–320 nm) and part of the UV-A region (320–372 nm). ZnO NPs have high absorption power of ultraviolet rays and can efficiently absorb them; they showed an intense absorption peak at 200–370 nm with very low diffuse reflectance (~4%). The band gap energy (Eg) of ZnO NPs was determined according to Kubelka-Munk function [49]:$F(R) = \frac{(1-R)^2}{2R}$ by plotting of $[F(R)h\nu]^{0.5}$ versus photon energy ($h\nu$) where $h\nu = \frac{1240}{\lambda}$, R is the diffuse reflectance data of ZnO NPs, h is Planck constant and λ is the absorption wavelength. The band gap ZnO NPs was calculated to be 3.16 eV which clearly confirm the ultraviolet radiation.

The parameters (EE(λ)×I(λ)) required to determine sun protection factor performance (SPF) values were shown in Table 1. EE(λ) values were according to those calculated by Sayre et al., 1979 [50], and the in vitro SPF value was calculated for ZnO NPs according to the Mansur method [38]. SPF has a set of numerical values in the range from 8 to 30 [51]. The SPF test was used to assess the capacity of synthesized ZnO NPs in absorbing UV radiation. The SPF value of ZnO NPs (SPF = 16.8) indicates more potential effectiveness of ZnO NPs as sunscreen in protecting the skin from the dangerous effects of UV rays. According to FDA guidelines, sunscreens with SPF ≥ 15 are able to prevent sunburn and reduce the risk of skin cancer and premature skin aging [52]. Therefore, synthesized ZnO NPs using SL juice are considered promising for further sunscreen formulations and personal care products.

3.3 Antioxidant Activity

The antioxidant activity of ZnO NPs synthesized with SL fruit extract was determined using DPPH free radicals. The DPPH solution has a deep violet color that gradually becomes pale yellow or colorless with the addition of increasing amounts of ZnO NPs allowing determination of the radical concentration [53]. The DPPH activity of the samples increased with increasing concentration of synthetic samples indicating a dose-dependent behavior. At concentrations 10–100 µg/mL, ZnO NPs showed a scavenging activity ranging from 13 to 75% with an average IC50 value, 51.91 ± 0.29 µg/mL. The antioxidant activity of ZnO NPs is lower than that of standard ascorbic acid (38–94%). Table 2 shows the effect of different concentrations of ZnO NPs and ascorbic acid on the DPPH radical antioxidant activity. The lower the scavenging activity value, the greater the ability of the samples to act as a DPPH scavenger. Compared with ascorbic acid at all concentrations from 10 to 100 µg/mL, the synthesized ZnO NPs are moderate free radical scavengers. The synthesized ZnO NPs showed scavenging activity ranging from 13 to 75% for concentrations from 10 to 100 µg/mL with an average IC50 value (51.91 ± 0.29). The relationship between the increases in DPPH activity of the ZnO NPs with an increase in its concentration indicates a dose-dependent behavior. The antioxidant properties of ZnO NPs arise due to the small particle sizes and can also arise from the transfer of electron density in O atoms, which depends on the structural arrangement of O atoms [51, 54]. Zinc plays an important role in many enzymes, both as a cofactor and as a component in redox processes and can reduce cell membrane damage and maintain the structure of the mitochondrial membrane from damage caused by free radicals generated by H_2O_2 from the body [55, 56].

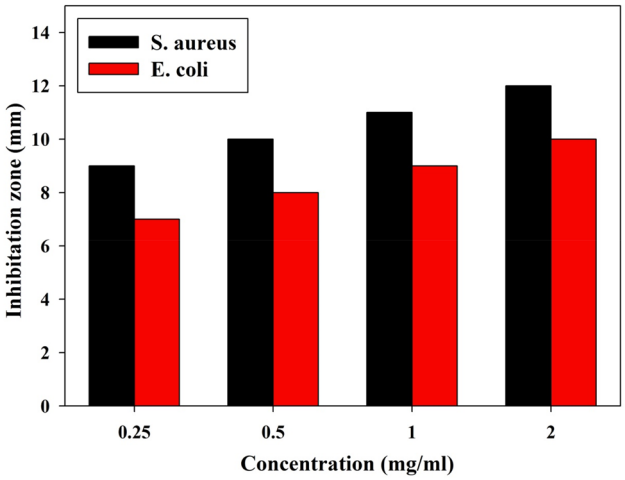

Fig. 7 Antibacterial activities of ZnO NPs at various concentrations (0.25, 0.5, 1, 2 mg/ml) and their level of zone of inhibition in mm

3.4 Antibacterial Activity

The antimicrobial efficacy of ZnO NPs prepared using SL juice was tested against two strains of pathogenic bacteria (*S. aureus* and *E. coli*). The antibacterial activity of ZnO NPs mainly depends on the particle size, the smaller the particle size, the higher its biological and chemical activity [57]. The synthesized ZnO NPs showed significant antibacterial activity on both bacterial strains as shown in Fig. 6. The growth inhibition affected by ZnO NPs against both positive and gram-negative organisms (*S. aureus* and *E. coli*) is shown in Fig. 7. The tested *S. aureus* strain showed higher sensitivity compared to the *Escherichia coli* strain at all concentrations of ZnO NPs. The diameter of inhibition zones was observed with the *S. aureus* strains (9 to 12 mm) followed by *E. coli* (7 to 10 mm). The exact mechanism behind the antibacterial effect of ZnO is still under discussion and study; One possible mechanism relies on electrostatic forces that lead

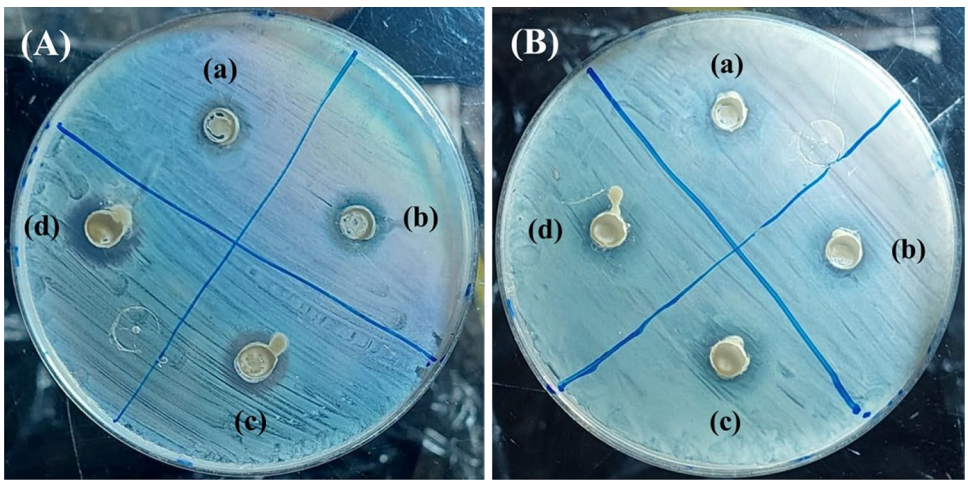

Fig. 6 The images of Petri dishes showing the antibacterial effects of synthesized ZnO NPs at different concentrations (a) 0.25 mg/ml, (b) 0.5 mg/ml, (c) 1.0 mg/ml, and (d) 2.0 mg/ml: **A** *S. aureus* and **B** *E. coli*

to direct bacterial killing as a result of the abrasive surface texture attachment of ZnO NPs to the bacterial surface [58], mechanical destruction of the bacterial cell membrane caused by ZnO NP penetration [59], and the release of Zn^{+2} ions from ZnO NPs [60], or formation of the active oxygen molecules [61].

3.5 Cell Culture and Cytotoxic Evaluations

The MTT results showed clear differences between the effect of ZnO NPs concentrations on normal WI-38 cells and cancerous HePG2 cells. Figure 8 shows that at concentrations up to 50 µg/mL, ZnO NPs did not show cytotoxic activity against normal WI-38 while they did not show cytotoxic activity against HePG2 cancer cells up to 6.25 µg/mL. At concentrations higher than 6.25 µg/mL, ZnO NPs significantly induced cell death in cancer cells (HePG2 cells) compared to normal cells (WI-38 cells). The MTT results showed an increase in the number of dead cells with increasing concentrations of ZnO NPs. Also, ZnO NPs had a better cell-killing effect on cancer cells than normal, which means that cancer cells were more sensitive to ZnO NPs. Although the mechanisms of cytotoxicity caused by ZnO NPs are not fully understood, production of reactive oxygen species (ROS) is thought to be a key factor [62]. ROS can be produced exogenously upon response to various stimuli including nanomaterials [63]. Cellular defense mechanisms are triggered when ZnO NPs interact with cells [64]. However, if the cell's ability to combat the production of ROS is exceeded, biomolecules are damaged by oxidation, which can lead to cell death [65]. Intrinsic cellular functions such as mitochondrial respiration, inflammatory response, microsome activity, and peroxisome activity all lead to ROS production [66]. Most of the studies using ZnO NPs synthesized using plant extracts showed their ability to stop the growth of cancer cells without having any negative effect on healthy cells [67]. Also, the anticancer activity of ZnO NPs was found to be dose dependent, with its activity peaking at higher doses [68, 69].

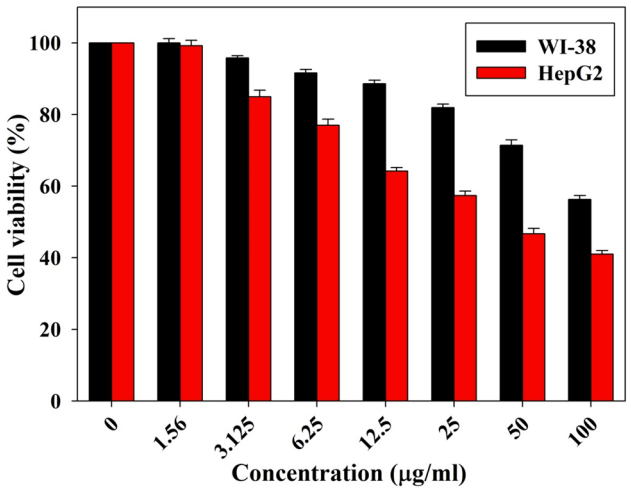

Fig. 8 Cell viability after 24 h. WI-38: Human lung fibroblasts (non-malignant cells) and HepG2: human hepatocellular carcinoma cell, have been treated with ZnO NPs

4 Conclusion

For the first time, SL juice has been used in the green synthesis of ZnO NPs for multifunctional sunscreen applications. SL fruit juice is an excellent, non-toxic source and can play a triple role by acting as a solvent, reducing agent and stabilizer which facilitates the synthesis of ZnO NPs. ZnO NPs have a pure crystal structure, and the particles have a quasi-spherical surface shape with a size of 39 ± 12 nm. On the one hand, ZnO NPs possess strong UV protection capability (in vitro SPF = 16.8), and thus they are an excellent candidate as UV filter material for sunscreen enhancement. On the other hand, ZnO NPs offer an extra approach as an antibacterial and anticancer material. Notably, ZnO NPs are moderate antioxidants and enhance the cytotoxic activity against (HePG2) tumor cells. In addition, ZnO NPs confirmed their efficacy against pathogens because they possess antibacterial activity against *S. aureus* and *E. coli*.

Acknowledgements The authors are greatly thankful to faculty of science Tanta University for support.

Author Contributions The samples were prepared by RM and AE, the results were interpreted. AE did all the laboratory measurements. All authors participated in writing and revising the manuscript.

Funding Open access funding provided by The Science, Technology & Innovation Funding Authority (STDF) in cooperation with The Egyptian Knowledge Bank (EKB). no funding.

Data Availability All data produced during this work are included in this published article.

Declarations

Competing Interests The authors declare no competing interests.

Ethical Approval This study does not involve any form of human participation or animal testing. Hence the ethical approval is not required. And I do not use any reproduced images.

References

1. R.N. Saladi, A.N. Persaud, The causes of skin cancer: a comprehensive review. Drugs Today **41**, 37–54 (2005)
2. P. Elsner, E. Hölzle, T. Diepgen, S. Grether-Beck, H. Hönigsmann, J. Krutmann et al., Recommendation: dailysun protection in the prevention of chronic UV-induced skin damage. JDDG J der Dtsch Dermatol. Ges. **5**, 166–73 (2007)
3. S.J. Balk, Council on Environmental Health and Section on Dermatology, Ultraviolet radiation: a hazard to children and adolescents. Pediatrics **127**, 588–597 (2011)
4. T.G. Smijs, S. Pavel, Titanium dioxide and zinc oxide nanoparticles in sunscreens: focus on their safety and effectiveness. Nanotechnol. Sci. Appl. **4**, 95 (2011)
5. P.K. Mishra, H. Mishra, A. Ekielski, S. Talegaonkar, B. Vaidya, Zinc oxide nanoparticles: a promising nanomaterial for biomedical applications. Drug Discov. Today **22**, 1825–1834 (2017)
6. R. Chauhan, A. Kumar, R. Tripathi, A. Kumar, Advancing of zinc oxide nanoparticles for cosmetic applications, in *Handbook of Consumer Nanoproducts*. (Springer, Singapore, 2022), pp.1–16
7. S. Harinee, K. Muthukumar, H.-U. Dahms, M. Koperuncholan, S. .Vignesh, Banu, biocompatible nanoparticles with enhanced photocatalytic and anti-microfouling potential. Int. Biodeterior. Biodegrad. **145**, 104790 (2019)
8. A. Farooq, M.K. Patoary, M. Zhang, H. Mussana, M. Li, Naeem, Cellulose from sources to nanocellulose and an overview of synthesis and properties of nanocellulose/zinc oxide nanocomposite materials. Int. J. Biol. Macromol. **154**, 1050–1073 (2020)
9. S.S. Ali, R. Morsy, N.A. El-Zawawy, M.F. Fareed, M.Y. Bedaiwy, Synthesized zinc peroxide nanoparticles (ZnO2-NPs): a novel antimicrobial, anti-elastase, anti-keratinase, and anti-inflammatory approach toward polymicrobial burn wounds. Int. J. Nanomed. **12**, 6059 (2017)
10. S.L. Schneider, H.W. Lim, A review of inorganic UV filters zinc oxide and titanium dioxide. Photodermatol. Photoimmunol. Photomed. **35**, 442–446 (2019)
11. K. Pal, S. Chakroborty, N. Nath, Limitations of nanomaterials insights in green chemistry sustainable route: review on novel applications. Green Process. Synth. **11**, 951–964 (2022)
12. S. Sagadevan, K. Pal, Z.Z. Chowdhury, E.M. Chowdhury, Hoque, Structural, dielectric and optical investigation of chemically synthesized Ag-doped ZnO nanoparticles composites. J. Solgel Sci. Technol. **83**, 394–404 (2017)
13. H. Agarwal, S.V. Kumar, S. Rajeshkumar, A review on green synthesis of zinc oxide nanoparticles–An eco-friendly approach. Resour. Technol. **3**, 406–413 (2017)
14. I.S. Asiya, K. Pal, S. Kralj, S.G. El-Sayyad, G.F. de Souza, T. Narayanan, Sustainable preparation of gold nanoparticles via green chemistry approach for biogenic applications. Mater. Today Chem. **17**, 100327 (2020)
15. N.V. Kalpana, V. Devi Rajeswari, A review on green synthesis, biomedical applications, and toxicity studies of ZnO NPs. Bioinorg. Chem. Appl. (2018). https://doi.org/10.1155/2018/3569758
16. R. Verma, S. Pathak, K.A. Srivastava, S. Prawer, S. Tomljenovic-Hanic, ZnO nanomaterials: green synthesis, toxicity evaluation and new insights in biomedical applications. J. Alloys Compd. **876**, 160175 (2021)
17. S. Ahmed, S.A. Chaudhry, S. Ikram, A review on biogenic synthesis of ZnO nanoparticles using plant extracts and microbes: a prospect towards green chemistry. J. Photochem. Photobiol. B Biol. **166**, 272–284 (2017)
18. S. Busi, J. Rajkumari, S. Pattnaik, P. Parasuraman, S. Hnamte, Extracellular synthesis of zinc oxide nanoparticles using Acinetobacter schindleri SIZ7 and its antimicrobial property against foodborne pathogens. J. Microbiol. Biotechnol. Food Sci. **05**, 407–411 (2016)
19. M.R. Tripathi, S.A. Bhadwal, K.R. Gupta, P. Singh, A. Shrivastav, R.B. Shrivastav, ZnO nanoflowers: novel biogenic synthesis and enhanced photocatalytic activity. J. Photochem. 35 Photobiol B Biol. **141**, 288–295 (2014)
20. E. Selvarajan, V. Mohanasrinivasan, Biosynthesis and characterization of ZnO nanoparticles using lactobacillus plantarum VITES07. Mater. Lett **112**, 180–182 (2013)
21. N.V. Kalpana, S.A.B. Kataru, N. Sravani, T. Vigneshwari, A. Panneerselvam, V. Devi, Rajeswari, Biosynthesis of zinc oxide nanoparticles using culture filtrates of Aspergillus niger: antimicrobial textiles and dye degradation studies. OpenNano. **3**, 48–55 (2018)
22. H. Kumar, R. Rani, Structural and optical characterization of ZnO nanoparticles synthesized by microemulsion route. Int. Lett. Chem. Phys. Astron **14**, 26–36 (2013)
23. S. Azizi, B.M. Ahmad, F. Namvar, R. Mohamad, Green biosynthesis and characterization of zinc oxide nanoparticles using brown marine macroalga sargassum muticum aqueous extract. Mater. Lett **116**, 275–277 (2014)
24. J.O. Nava, A.P. Luque, M.C. Gómez-Gutiérrez, R.A. Vilchis-Nestor, A. Castro-Beltrán, L.M. MotaGonzález, A. Olivas, Influence of Camellia sinensis extract on Zinc Oxide nanoparticle green synthesis. J. Mol. Struct. **1134**, 121–125 (2017a)
25. M. Fazlzadeh, R. Khosravi, A. Zarei, Green synthesis of zinc oxide nanoparticles using peganum harmala seed extract, and loaded on peganum harmala seed powdered activated carbon as new adsorbent for removal of cr(VI) from aqueous solution. Ecol. Eng **103**, 180–190 (2017)
26. S. Gunalan, R. Sivaraj, V. Rajendran, Green synthesized ZnO nanoparticles against bacterial and fungal pathogens. Prog. Nat. Sci. Mater. Int. **22**, 693–700 (2012)
27. P. Sutradhar, M. Saha, Green synthesis of zinc oxide nanoparticles using tomato (lycopersicon esculentum) extract and its photovoltaic application. J. Exp. Nanosci **11**, 314–327 (2017)
28. K. Ranoszek-Soliwoda, E. .Tomaszewska, K. Małek, G. Celichowski, P. .Orlowski, M. .Krzyzowska, The synthesis of monodisperse silver nanoparticles with plant extracts. Colloids Surf. B Biointerfaces. **177**, 19–24 (2019)
29. V.V. Makarov, J.A. Love, V.O. Sinitsyna, S.S. Makarova, V.I. Yaminsky, E.M. Taliansky, "Green" nanotechnologies: synthesis of metal nanoparticles using plants. Acta Naturae (англоязычная версия) **6**, 35–44 (2014)
30. R.H. Dihom, M.M. Al-Shaibani, R.S.M.R. Mohamed, A.A. Al-Gheethi, A. Sharma, B.H.M. Khamidun, Photocatalytic degradation of disperse azo dyes in textile wastewater using green zinc oxide nanoparticles synthesized in plant extract: a critical review. J. Water Process. Eng. **47**, 102705 (2022)
31. A. Bukhari, I.I. Gilani, A. Nazir, H. Zain, R. Saeed, Green synthesis of metal and metal oxide nanoparticles using different plants' parts for antimicrobial activity and anticancer activity: a review article. Coatings **11**, 1374 (2021)
32. N.A.I.M. Ishak, S.K. Kamarudin, S.N. Timmiati, Green synthesis of metal and metal oxide nanoparticles via plant extracts: an overview. Mater. Res. Express. **6**, 112004 (2019)

33. R.A. Prasad, L. Williams, J. Garvasis, O.K. Shamsheera, M.S. Basheer, M. Kuruvilla, Applications of phytogenic ZnO nanoparticles: a review on recent advancements. J. Mol. Liq. **331**, 11 (2021)
34. P. Khandel, R.K. Yadaw, D.K. Soni, L. Kanwar, S.K. Shahi, Biogenesis of metal nanoparticles and their pharmacological applications: present status and application prospects. J. Nanostructure Chem. **8**, 217–254 (2018)
35. M. Kumar, M. Tomar, J.D. Bhuyan, S. Punia, S. Grasso, A.G.A. Sa, Tomato (*Solanum lycopersicum* L.) seed: a review on bioactives and biomedical activities. Biomed. Pharmacother. **142**, 112018 (2021)
36. M. Mirahmadi, S. Azimi-Hashemi, E. Saburi, H. Kamali, M. Pishbin, F. Hadizadeh, Potential inhibitory effect of lycopene on prostate cancer. Biomed. Pharmacother. **129**, 110459 (2020)
37. J.P. Islamian, H. Mehrali, Lycopene as a carotenoid provides radioprotectant and antioxidant effects by quenching radiation-induced free radical singlet oxygen: an overview. Cell. J. **16**, 386 (2015)
38. O.T. Ademosun, A.H. Adebayo, K.O. Ajanaku, Solanum lycopersicum and Daucus carota: effective anticancer agents (a mini review). J. Phys.: Conf. Ser. **1943**, 12169 (2021)
39. S.J. MANSUR, R.N.M. BREDER, A.C.M. MANSUR, D.R. AZULAY, Determinação do fator de proteção solar por espectrofotometria. An. Bras. Dermatol. Rio de Janeiro. **61**, 121–124 (1986)
40. R. Soni, M. Sihag, N. Rani, M. Kinger, K.D. Aneja, Aqueous mediated reactions involving hypervalent iodine reagents. Asian J. Org. Chem. **11**, e202200125 (2022)
41. L. Yegrem, L.A. Dagnaw, Pretreatments, dehydration methods and packaging materials: effects on the nutritional quality of tomato powder. Austin J. Nutri Food Sci **102**, 1167 (2022)
42. J. Jeevanandam, F. Kiew, S. Boakye-Ansah, Y.S. Lau, A. Barhoum, Danqua., Green approaches for the synthesis of metal and metal oxide nanoparticles using microbial and plant extracts. Nanoscale. **14**, 2534–2571 (2022)
43. T. Karnan, S.A.S. Selvakumar, Biosynthesis of ZnO nanoparticles using rambutan (*Nephelium lappaceum* L.) peel extract and their photocatalytic activity on methyl orange dye. J. Mol. Struct. **1125**, 358–365 (2016)
44. B. Bocca, S. Caimi, O. Senofonte, A. Alimonti, F. Petrucci, ICP-MS based methods to characterize nanoparticles of TiO2 and ZnO in sunscreens with focus on regulatoryandsafetyissues. Sci. Total Environ. **630**, 922–930 (2018)
45. S.H. Khoreem, A.H. AL-Hammadi, W.F. Al-Eryani, FTIR Spectra Analysis of Zinc Substituted Barium Nickel Ferrite. (2022)
46. T. Thangeeswari, A.T. George, A.A. Kumar, Optical properties and FTIR studies of cobalt doped ZnO nanoparticles by simple solution method. Indian J. Sci. Technol. **9**(1), 1–4 (2016)
47. V. Srivastava, D. Gusain, Y.C. Sharma, Synthesis, characterization and application of zinc oxide nanoparticles (n-ZnO). Ceram. Int. **39**, 9803–9808 (2013)
48. G. Bisht, S. Rayamajhi, B. Kc, S.N. Paudel, D. Karna, B.G. Shrestha, Synthesis, characterization, and study of in vitro cytotoxicity of ZnO-Fe3O4 magnetic composite nanoparticles in human breast cancer cell line (MDA-MB-231) and mouse fibroblast (NIH 3T3). Nanoscale Res. Lett. **11**, 1–11 (2016)
49. E. Darezereshki, Synthesis of maghemite (γ-Fe2O3) nanoparticles by wet chemical method at room temperature. Mater. Lett. **64**, 1471–1472 (2010)
50. G. Kortüm, *Reflectance Spectroscopy: Principles, Methods, Applications* (Springer, New York, 1969)
51. D. Das, C.B. Nath, P. Phukon, A. Kalita, K.S. Dolui, Synthesis of ZnO nanoparticles and evaluation of antioxidant and cytotoxic activity. Colloids. Surf. B. Biointerfaces **111**, 556–560 (2013)
52. A.E. Dutra, C.D.G.A.D. Oliveira, M.R.E. Kedor-Hackmann, M.R.I.M. Santoro, Santoro, Determination of sun protection factor (SPF) of sunscreens by ultraviolet spectrophotometry. Rev. Bras. Cienc. Farm. **40**, 381–385 (2004)
53. Q.S. Wang, W.H. Lim, Current status of the sunscreen regulation in the United States: 2011 food and drug administration's final rule on labeling and effectiveness testing. J. Am. Acad. Dermatol. **65**, 863–869 (2011)
54. M. Stan, A. Popa, D. Toloman, T.-D. Silipas, D.C. Vodnar, Antibacterial and antioxidant activities of ZnO nanoparticles synthesized using extracts of Allium sativum, Rosmarinus officinalis and Ocimum basilicum. Acta. Metall. Sin. (Engl. Lett.) **29**, 228–236 (2016)
55. G. Rajakumar, M. Thiruvengadam, G. Mydhili, T. Gomathi, I.M. Chung, Green approach for synthesis of zinc oxide nanoparticles from *Andrographis paniculata* leaf extract and evaluation of their antioxidant, anti-diabetic, and anti-inflammatory activities. Bioprocess Biosyst. Eng. **41**, 21–30 (2018)
56. A.W. Alshameri, M. Owais, Antibacterial and cytotoxic potency of the plant-mediated synthesis of metallic nanoparticles Ag NPs and ZnO NPs: a review. OpenNano **8**, 100077 (2022)
57. P.K. Stoimenov, R.L. Klinger, G.L. Marchin, Klabunde,Metal oxide nanoparticles as bactericidal agents. Langmuir. **18**, 6679–6686 (2002)
58. R. Hänsch, R.R. Mendel, Physiological functions of mineral micronutrients (cu, Zn, Mn, Fe, Ni, Mo, B, cl). Curr. Opin. Plant. Biol. **12**, 259–266 (2009)
59. C.-Y. Zhao, S.-X. Tan, X.-Y. Xiao, X.-S. Qiu, J.-Q. Pan, Z.-X. Tang, Effects of dietary zinc oxide nanoparticles on growth performance and antioxidative status in broilers, Biol. Trace Elem. Res. **160**, 361–367 (2014)
60. R. Brayner, R. Ferrari-Iliou, N. Brivois, S. Djediat, M.F. Benedetti, F. Fiévet, Toxicological impact studies based on Escherichia coli bacteria in ultrafine ZnO nanoparticles colloidal medium. Nano. Lett. **6**, 866–870 (2006)
61. M. Heinlaan, A. Ivask, I. Blinova, H.-C. Dubourguier, A. Kahru, Toxicity of nanosized and bulk ZnO, CuO and TiO2 to bacteria Vibrio fischeri and crustaceans Daphnia magna and Thamnocephalus platyurus. Chemosphere **71**, 1308–1316 (2008)
62. T. Xu, C.S. Xie, Tetrapod-like nano-particle ZnO/ acrylic resin composite and its multi-function property. Prog. Org. Coat. **46**, 297–301 (2003)
63. C.T. Ng, Q.L. Yong, P.M. Hande, N.C. Ong, E.L. Yu, H.B. Bay, H.G. Baeg, Zinc oxide nanoparticles exhibit cytotoxicity and genotoxicity through oxidative stress responses in human lung fibroblasts and Drosophila melanogaster. Int. J. Nanomed. (2017). https://doi.org/10.2147/ijn.s124403
64. A. Manke, L. Wang, Y. Rojanasakul, Mechanisms of nanoparticle-induced oxidative stress and toxicity. Biomed. Res. Int. **15**, 88 (2013)
65. M. Saliani, R. Jalal, E.K. Goharshadi, Mechanism of oxidative stress involved in the toxicity of ZnO nanoparticles against eukaryotic cells. Nanomed. J. **3**(1), 1–14 (2016)
66. R.J. Carmody, T.G. Cotter, Signaling apoptosis: a radical approach. Redox Rep. **6**, 77–90 (2001)
67. G. Bisht, S. Rayamajhi, ZnO nanoparticles: a promising anticancer agent. Nanobiomedicine. **3**, 3–9 (2016)
68. S. Zeghoud, H. Hemmami, B.B. Seghir, I.B. Amor, I. Kouadri, A. Rebiai, J. Simal-Gandara, A review on biogenic green synthesis of ZnO nanoparticles by plant biomass and their applications. Mater. Today Commun. **33**, 104747 (2022)
69. S.E. González, E. Bolaina-Lorenzo, J.J. Pérez-Trujillo, B.A. Puente-Urbina, O. Rodríguez-Fernández, A. Fonseca-García, R. Betancourt-Galindo, , Antibacterial and anticancer activity of ZnO with different morphologies: a comparative study. 3 Biotech **11**, 1–12 (2021)